NRIAG Journal of Astronomy and Geophysics 7 (2018) 201–207

Contents lists available at ScienceDirect

NRIAG Journal of Astronomy and Geophysics

journal homepage: www.elsevier.com/locate/nrjag

Full length article

# Investigation of structural and electrical properties of ZnO varistor samples doped with different additives

M.M. Saadeldin[a], Osama A. Desouky[b], Makram Ibrahim[c], G.E. Khalil[d], M.Y. Helali[c,*]

[a] Physics Department, Faculty of Science, Cairo University, Egypt
[b] Higher Institute of Engineering, Ministry of Higher Education, Belbes, Egypt
[c] Space Research Lab, National Research Institute of Astronomy and Geophysics, Egypt
[d] National Institute of Laser Enhanced Science, NILES, Cairo University, Egypt

ARTICLE INFO

*Keywords:*
ZnO
CuO
SEM
EDX
AFM
Conductivity

ABSTRACT

Three samples of ZnO doped with CuO as additive were prepared by solid state reaction from the calcined oxides and characterized by SEM, EDX, and AFM. The results revealed the presence of intergranular phase. Additives found to be between ZnO grains. The conductivity of the three samples was measured with the frequency up to 100 KHz by LCR circuit. The calculated coefficients of nonlinearity and the conductivity are shown to be highly dependent on the frequency, concentration of copper oxide, surface morphology, and microstructure of the varistor samples. The temperature dependence of the conductivity of these samples will be studied in the future work.

## 1. Introduction

ZnO is a wide band gap semiconductor material with numerous important present applications such as optoelectronic devices and varistors (Gupta, 1840; Vandal Pol, 1990), surface acoustic wave devices, UV light-emitting diodes, transparent field-effect transistors, facial powders, piezoelectric transducers, transparent conducting films (Clarke, 1999; Greuter and Blatter, 1990), and gas sensors (Matsuoka, 1971; Matsuoka et al., 1970). However, all of these applications are either dependent upon, or are affected by the impurities and defects. As varistors, they are widely used in electrical circuits against dangerous voltage surges. Zinc oxide crystallizes in the hexagonal wurtzite lattice (Yoshitsugu et al., 1988) in which the oxygen ions are arranged in closest hexagonal packing and the zinc ions occupy half of the tetrahedral interstitial positions and have the same relative arrangement as the oxygen ions. Metal Oxide varistors were initially developed in Japan (Matsuoka, 1971). ZnO varistors are highly complex, multicomponent, polycrystalline oxide ceramics devices with highly nonlinear current-voltage characteristics whose electrical behavior depends both on the microstructure of the device and on detailed processes occurring at the ZnO grain boundaries. The primary constituent of such a varistor is obviously ZnO, typically 90% or more. In addition to this the varistor contains smaller amounts of other constituents. These voltage suppressors are characterized by non-linear V-I relation (1), this holds particularly true for the applied electrical processes which take place on the grain boundaries of the ZnO crystals (Steele, 1993). The deviation from Ohm's law is shown in Fig. 1 (Matsuoka et al., 1970). This property is related to the conduction mechanism in the intergranular phase which is related to the electronic structure in the vicinity of the grain boundaries.

It is assumed that oxygen atoms are oriented at ZnO grain boundaries; these oxygen atoms are responsible for the generation of the electronic states out of the grain boundaries. Schottky barriers are formed on both sides of the grain boundary where a depletion layer is formed as a result within the ZnO grains, and this depletion layer controls the varistor action. Therefore, conduction paths are located between grains in the region of closest contact over the Schottky barrier as well as through bulk intergranular material at grain corners. The former may show a thermally activated temperature leakage conduction related to barrier height while the latter is thermally sensitive but is governed by the additives.

The voltage – current characteristics of ZnO varistors are expressed approximately by:

$$I = (V/C)^{\alpha} \quad (1)$$

where

V: is the voltage across the sample.
I: is the current flowing through the sample.

Peer review under responsibility of National Research Institute of Astronomy and Geophysics.

* Corresponding author.
*E-mail address:* mohelaly71@gmail.com (M.Y. Helali).

https://doi.org/10.1016/j.nrjag.2018.06.002
Received 19 March 2017; Received in revised form 9 June 2018; Accepted 30 June 2018
Available online 04 July 2018

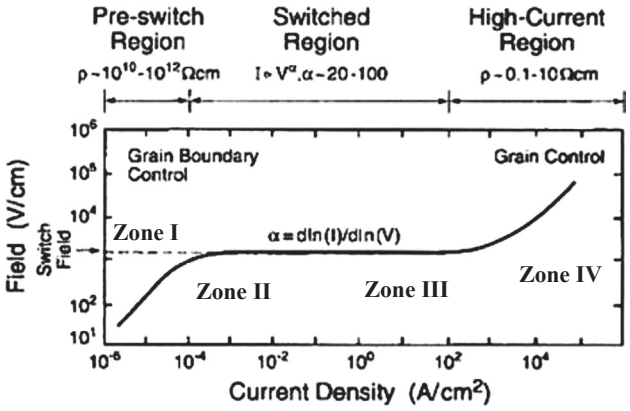


**Fig. 1.** V-I characteristics of ZnO – Varistors.

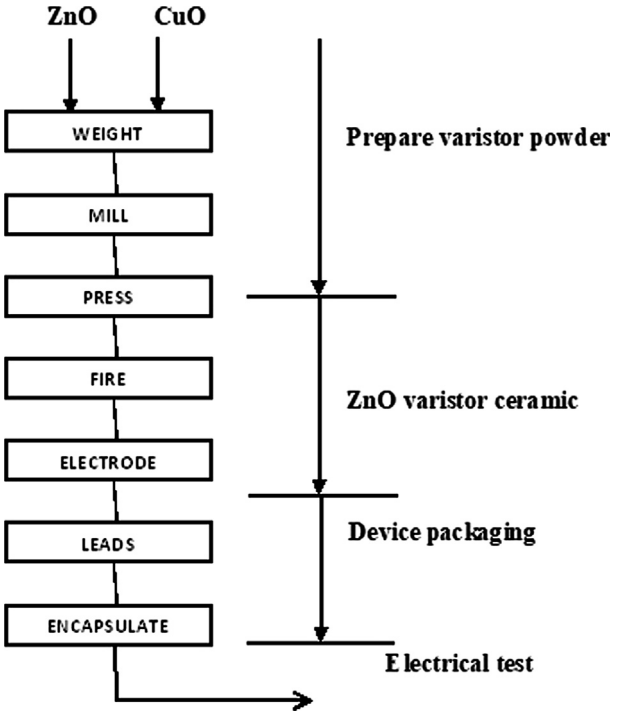


**Fig. 2.** A block diagram to show different stages of preparation of the ZnO samples.

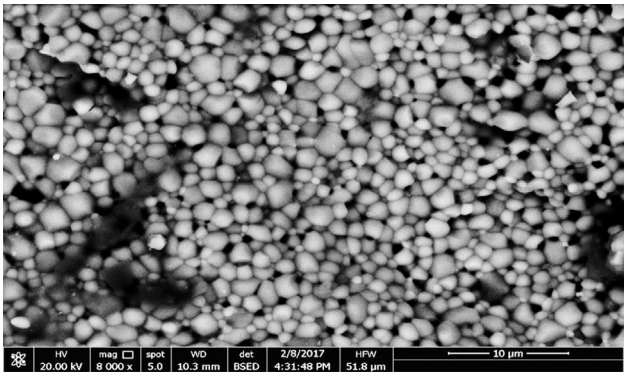

**Fig. 3a.** SEM image of sample M2, General view, with magnification 8000.

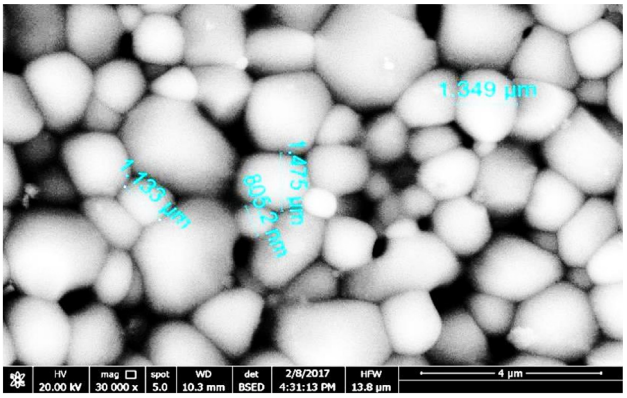


**Fig. 3b.** SEM image of sample M2 with 4 sample grain diameter measurements, with magnification 30,000.

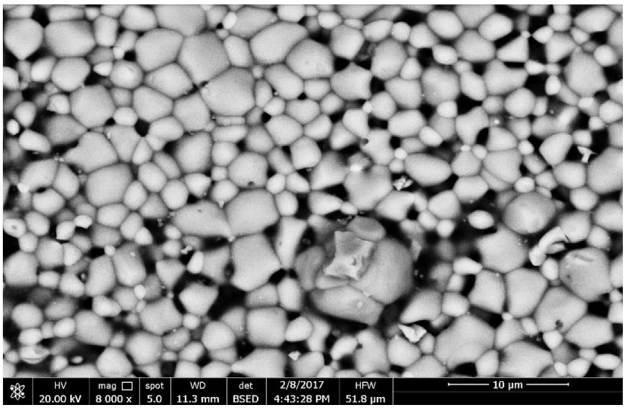

**Fig. 4a.** SEM image of sample M3, with magnification 8000.

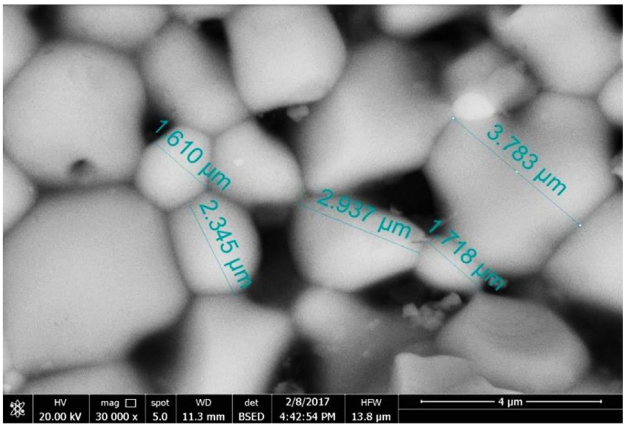


**Fig. 4b.** SEM image of sample M3, with magnification 30,000.

C: is a constant, and α is a nonlinearity parameter.

The V-I curve in Fig. 1 of a ZnO varistors can be divided into three important regions (Matsuoka et al., 1970):

Low- current linear region, below the threshold voltage (typically a voltage at hundreds of μA/cm$^2$).
Intermediate nonlinear region, between the threshold voltage and voltage at a current of about $10^2$–$10^3$ A/cm$^2$, the (V-I) characteristic in this region is almost independent of temperature (Machlen, 1979).
High- current linear region, above approximately $10^3$ A/cm$^2$.

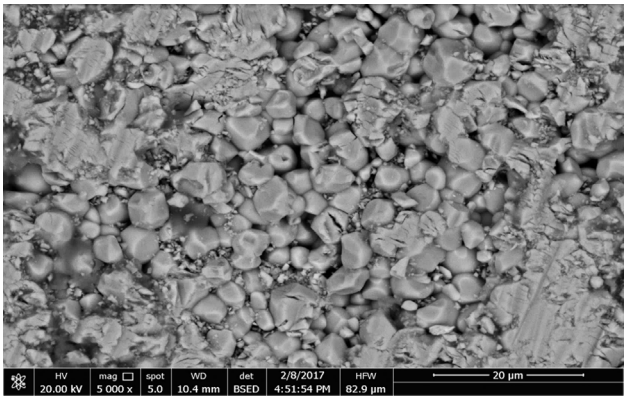


**Fig. 5a.** SEM image of sample M5, with magnification 5000.

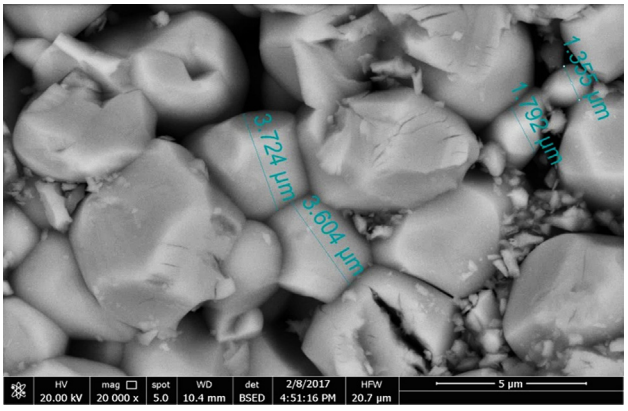


**Fig. 5b.** SEM image of sample M5, with magnification 20,000.

The nonlinearity parameter (α) is calculated from the following equation:

$$a = [\log I_2 - \log I_1]/[\log V_2 - \log V_1] \quad (2)$$

where $V_1$ and $V_2$ are the voltages at currents of $I_1$ and $I_2$, respectively (Chiou and Ji, 1986). Typical values for the exponent of non-linearity α, defined by $I \propto V^{\alpha}$, lie in the region $2 \leq \alpha \leq 6$, which is similar to the nonlinearity exhibited by Cerva and Russwurm (1988). A series of multicomponent ZnO based ceramic varistors with properties greatly superior to those attained on the binary systems have been developed by Jokemura et al. (1986), Matsuoka et al. (1970). These varistors, and those presently produced by General Electrical (Levinson and Philipp, 1975) under the trade name GE-MOV™, possess an extremely high nonlinearity in their current – voltage characteristic ($30 \leq \alpha \leq 50$) and are characterized by an excellent energy absorbing capacity.

## 2. Experimental work

Three ZnO disc samples of diameters 1.3 cm and thickness 0.2 cm doped with different amounts of CuO were prepared by the method described in the following subsection, and as shown in Fig. 2 which is a block diagram explaining the different stages of preperation of the samples. The other next part of the experimental work consists of the characterization of the three prepared samples using SEM, EDX, and AFM tools, and measuring of the conductivity using Hitester LCR system with frequency change from 1 Hz up to 100 KHz.

### 2.1. Sample preparation

The sintered polycrystalline samples were prepared by conventional ceramic fabrication procedures. Reagent – grade ZnO and CuO powders were mixed by wet ball – milling using deionized water. 3 Disc specimens with the following dimensions, diameter 1.3 cm and thickness 0.2 cm were processed under a force of 70 KN, dried and then fired at 1100C for 30 min.

Specimens were first polished with different grades of diamond past thoroughly washed in an ultrasonic bath, dried and then thermally etched. The CuO amount (measured in mol%) in the three sample are as follows; 0.5 mol% in sample M2, 1.0 mol% in sample M3, and 3.0 mol% in sample M5.

### 2.2. Scanning electron microscopy

SEM images and EDX of the three samples were carried out at the National Research Center using the Czech apparatus for SEM and EDX model: Quanta FEG 250. The resulting SEM images in Figs. 3, 4, and 5 are for the samples M2, M3, and M5 respectively. They show the detailed surface morphology, the presence of intergranular phase, and the CuO presence in grain boundaries (Desouky, 2015; Saadeldin et al., 2015) between the ZnO grains are very clear. And, comparing images for samples M2 and M3, Figs. 3 and 4, shows that increasing CuO from 0.5 mol% in sample M2 to 1 mol% in M3 causes an increase in the grain size in sample M3 than that of M2 which indicates a decrease in the distortion parameter.

The SEM shows ZnO grain of various sizes (about 2–5 µm). Submicron pores occur at triple points at the grain corners, which ZnO-

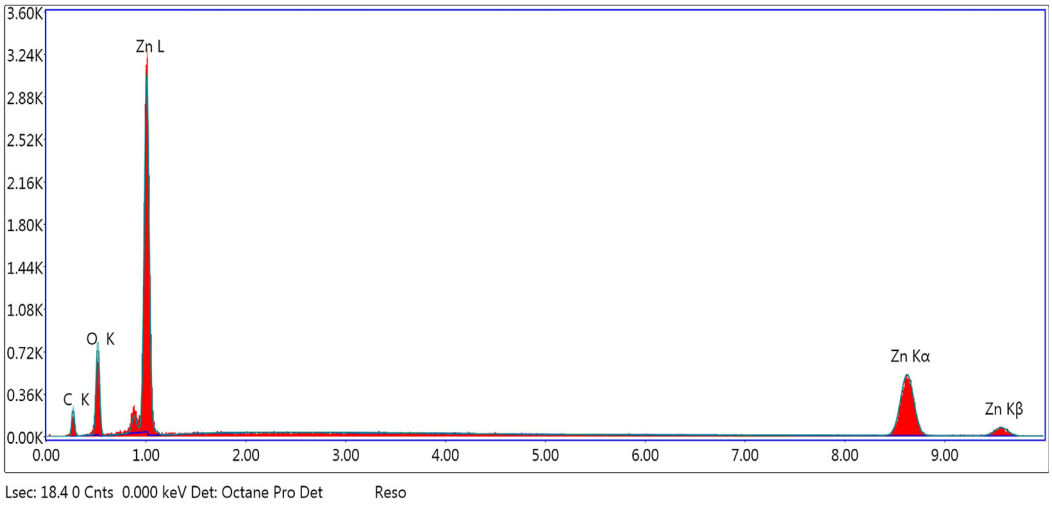


**Fig. 6.** EDX chart of the sample M2, showing the peaks of main constituents.

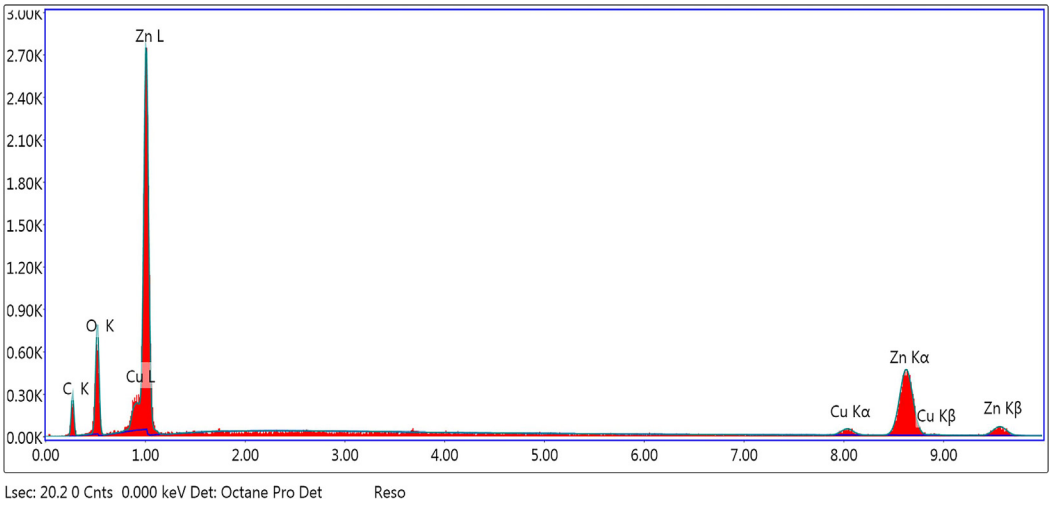


**Fig. 7.** EDX chart of the sample M3, showing the peaks of main constituents.

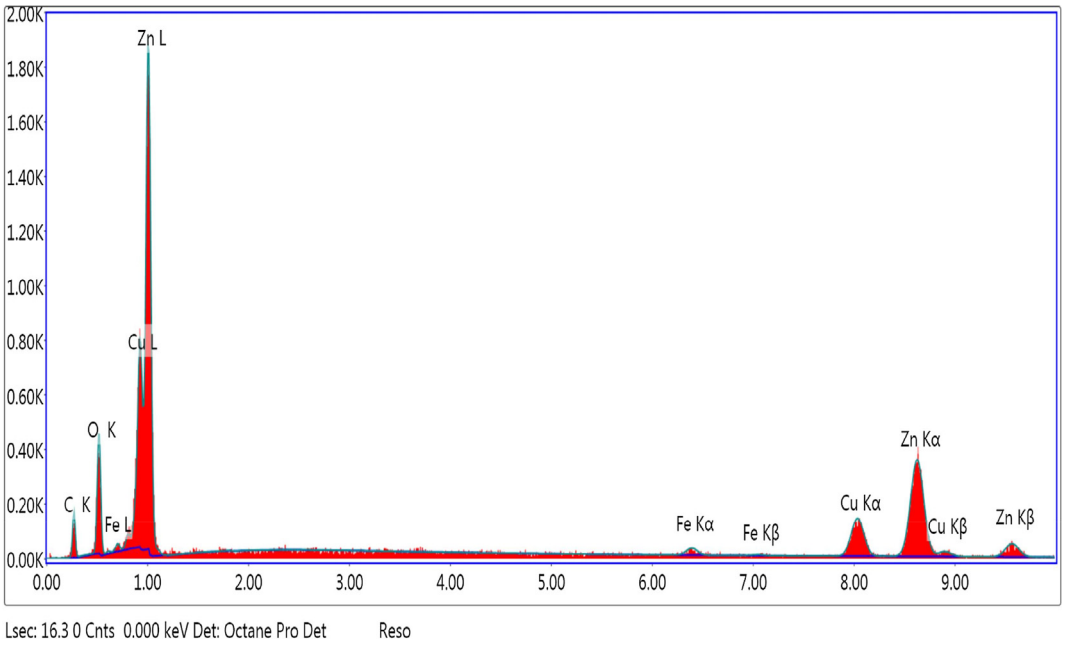


**Fig. 8.** EDX chart of sample M5, showing the peaks of its main constituents.

**Table 1**
Weight and atomic percents, net intensity and error percent of the main constituents of Sample M2.

| Element | Weight % | Atomic % | Net Int. | Error % |
|---|---|---|---|---|
| C | 15.56 | 37.3 | 40.82 | 14.03 |
| O | 18.76 | 33.77 | 177.4 | 10.34 |
| Zn | 65.68 | 28.93 | 453.32 | 3.15 |

**Table 2**
Weight and atomic percents, net intensity and error percent of the main constituents of Sample M3.

| Element | Weight % | Atomic % | Net Int. | Error % |
|---|---|---|---|---|
| C | 18.57 | 41.82 | 47.39 | 12.95 |
| O | 19.13 | 32.35 | 162.06 | 10.38 |
| Cu | 4 | 1.7 | 33.41 | 15.35 |
| Zn | 58.31 | 24.13 | 369.56 | 3.43 |

**Table 3**
Weight and atomic percents, net intensity and error percent of the main constituents of Sample M5.

| Element | Weight % | Atomic % | Net Int. | Error % |
|---|---|---|---|---|
| C | 13.8 | 37.15 | 32.73 | 14.81 |
| O | 13 | 26.28 | 114.24 | 11.51 |
| Fe | 1.29 | 0.75 | 20.96 | 23.54 |
| Cu | 16.25 | 8.27 | 130.24 | 6.13 |
| Zn | 55.66 | 27.54 | 349.1 | 3.61 |

**Table 4**
Average values of mean radius, maximum diameter, perimeter, distortion coefficient, and roughness for the three samples.

| Sample | Mean radius (μm) | Max. diameter (μm) | Perimeter (μm) | Distortion coefficient | Roughness |
|---|---|---|---|---|---|
| M2 | 0.08 | 0.249 | 0.622 | 0.739 | 1.586 |
| M3 | 0.092 | 0.306 | 0.737 | 0.548 | 1.885 |
| M5 | 0.083 | 0.233 | 0.623 | 0.769 | 1.326 |

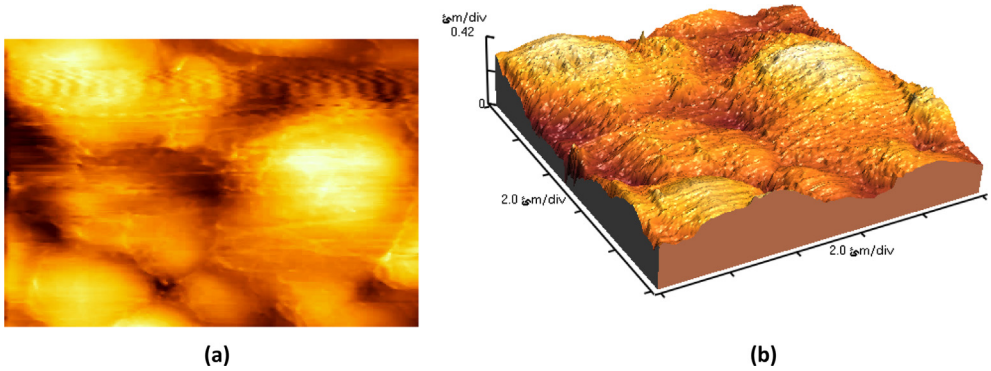


**Fig. 9.** the AFM images for the sample M2; two dimensional in (a) and three dimensional in (b), with surface area of 108.0 $\mu m^2$, volume of 53.77 $\mu m^3$, and with projected Area of 100.0 $\mu m^2$.

ZnO grain junctions are devoid of them. The high periodicity and grain hexagonal structure are clear for all samples from images in Figs. 3–5.

### 2.3. EDX

EDX Charts in Figs. 6, 7, and 8 show sharp peaks of the main constituents of samples M2, M3, and M5 respectively. Zn atoms are highly observed, all samples are polycrystalline, carbon and oxygen are observed in all samples while copper is not detectable in sample M2, Fig. 6, but observed in samples M3, Fig. 7, and M5, Fig. 8 in increasing abundance.

The Tables 1, 2, and 3, associated with the EDX charts for each sample in Figs. 6, 7, and 8 respectively, shows the weight percent, atomic percent, net intensity, and error for each detected element.

### 2.4. Atomic force microscopy

For collecting AFM data from the three samples, a contact-mode atomic force microscope model: Autoprobe cp-research head manufactured by Thermo microscope was used. The AFM data generate quantitative information from individual particles and between groups of particles which can allow precise analyses of maximum diameter, mean radius, perimeter, surface area, volume, distortion and roughness for each particle. The probe is a nonconductive silicon nitride, manufactured by Bruker. Model: MLCT-MT-A. And Proscan 1.8 software was used for controlling the scan parameters and IP 2.1 software was used for image analysis, the scan area was $10 \times 10\,\mu^2$ and the number of data points was 256 * 256 with scan rate of 1 Hz. Average mean radius, maximum diameter, perimeter, distortion coefficient, and roughness for the three samples from AFM data are shown in Table 4.

The AFM images in Figs. 9–11, and Table 4 for the three samples reveals the change in some surface morphology parameters such as the grain size for the three samples according to the percentage of CuO, and therefore a different surface morphology parameters as well between the three samples which is clear from values of mean radii, maximum diameters, perimeters, distortion coefficients, and roughness values for the three samples.

Figs. 12, 13, and 14 show the statistical distribution analyses of the mean radii of the particles versus the maximum diameters and histograms of number of particles for each maximum diameter interval for samples M2, M3, and M5 respectively.

The statistical distributions of the mean radii with maximum diameters in Figs. 12–14 show that the slowest rate of increase of the mean radius with maximum diameters belongs to sample M5 which contains the highest CuO concentration while the fastest rate of increase belongs to the sample M2 with the lowest CuO concentration. Also the histograms show that the maximum diameters of the sample M2 is about 1.8 µm, while for samples M3 and M5 less than or equal to 1.2 µm.

### 2.5. Conductivity and nonlinearity

The following electrical properties were determined for the three specimens fired at 1100 °C for two hours. The calculated (α) for the ZnO ceramic samples ranges from 45.6 to 54.8, achieving maximum 54.8 for the sample M5 with CuO content of 3 mol %, for M3 it was 49.5. The value of (α) increases with increasing CuO content for the three samples. It is clear that the ZnO sample M5, doped with 3 mol% CuO and small amounts of other additives should exhibit the best nonlinear properties as a varistor. So, it could be concluded that by adding more CuO the non-linear properties increase.

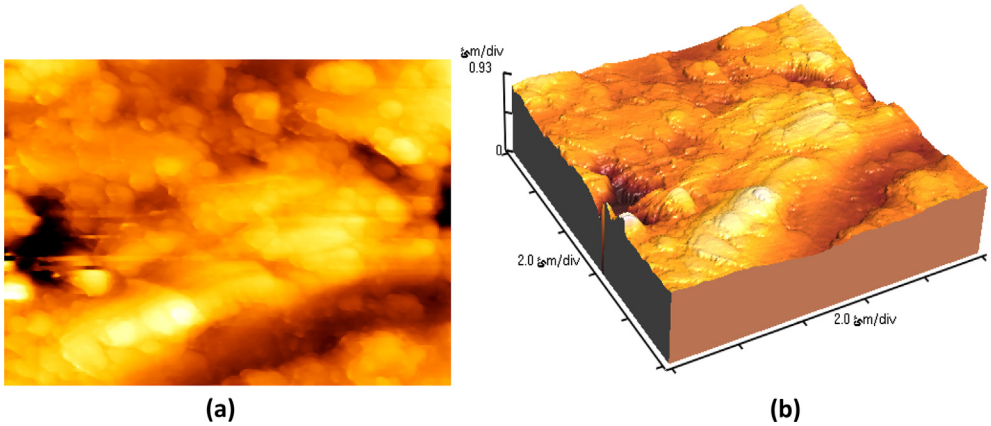


**Fig. 10.** The AFM images for the sample M3; two dimensional in (a) and three dimensional in (b), with surface area of 110.2 $\mu m^2$, volume of 150.0 $\mu m^3$, and with projected Area of 100.0 $\mu m^2$.

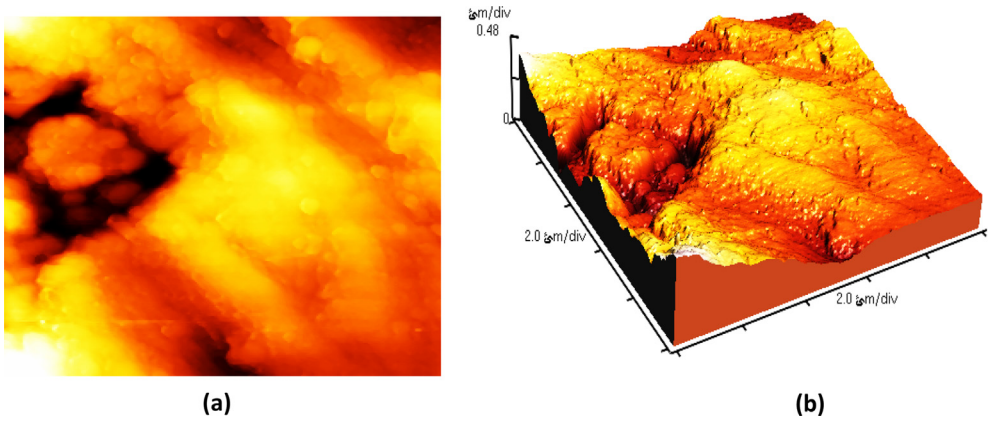


**Fig. 11.** The AFM images for the sample M5; two dimensional in (a) and three dimensional in (b), with surface area of 104.8 μm$^2$, volume of 46.15 μm$^3$, and with projected Area of 100.0 μm$^2$.

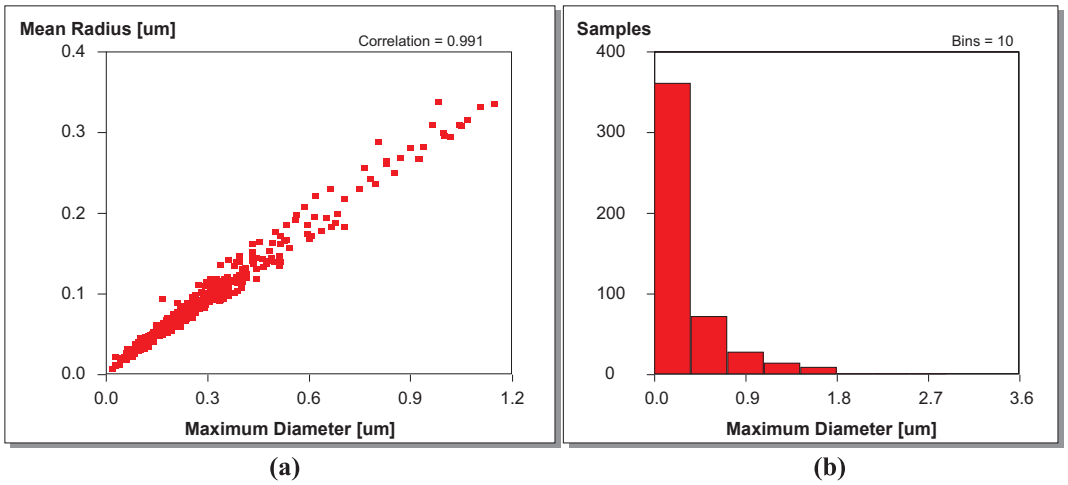


**Fig. 12.** Statistical distribution of mean radius with maximum diameter in (a), and histogram of number of samples with maximum diameter in (b) for sample M2.

Figs. 15 and 16 show the relations between conductivity (σ) and frequency at room temperature for samples M3 and M5 respectively in the frequency range from 1 Hz to 100 KHz. The results showed increase in the conductivity as the frequency increases. Also comparison between conductivities of different compounds represent increase in values of (σ) by increasing concentration of additives at frequencies above the breakdown which is around 1 KHz. The relation between conductivity and frequency shows that different samples behave differently according to the amount of CuO dopant added, therefor it is expected that the dielectric constant increases with frequency as well.

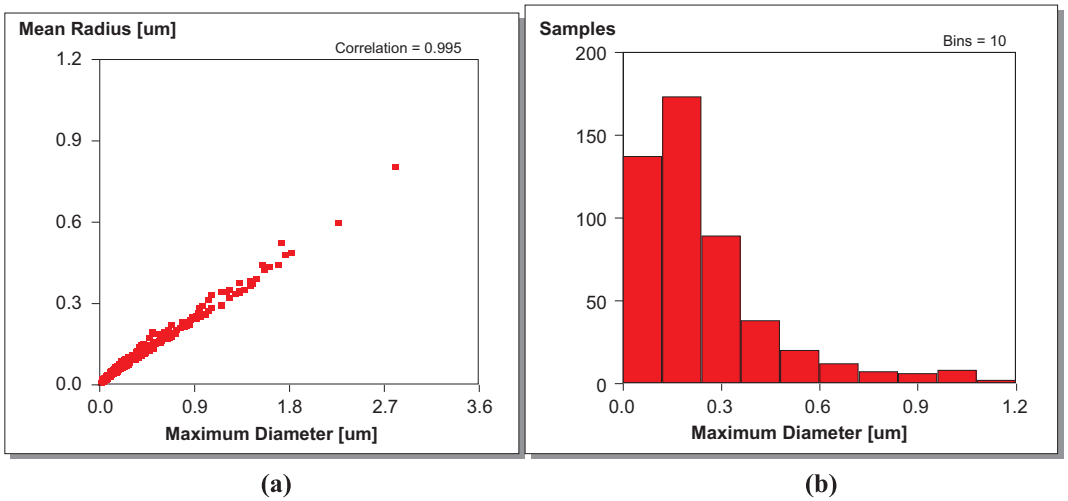


**Fig. 13.** Statistical distribution of mean radius with maximum diameter in (a), and histogram of number of samples with maximum diameter in (b) for sample M3.

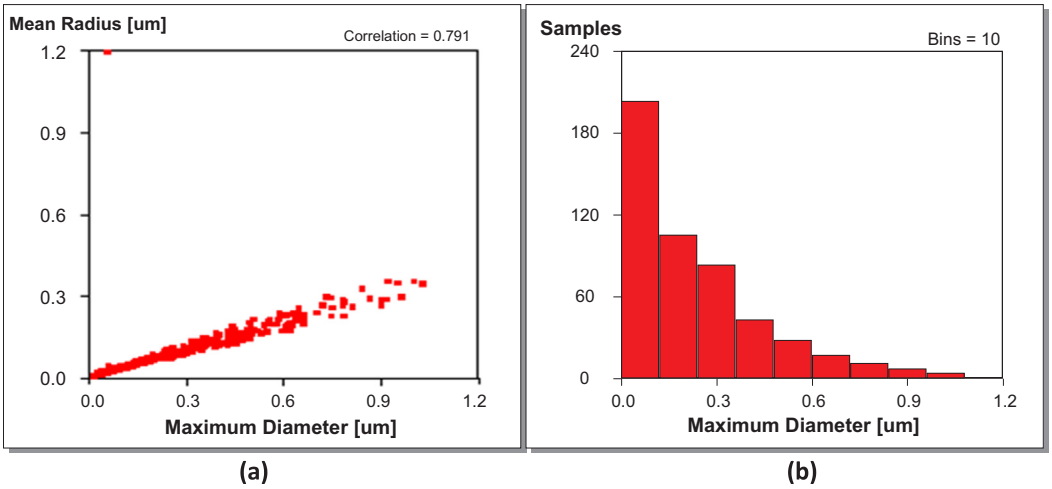


**Fig. 14.** Statistical distribution of mean radius with maximum diameter in (a), and histogram of number of samples with maximum diameter in (b) for sample M5.

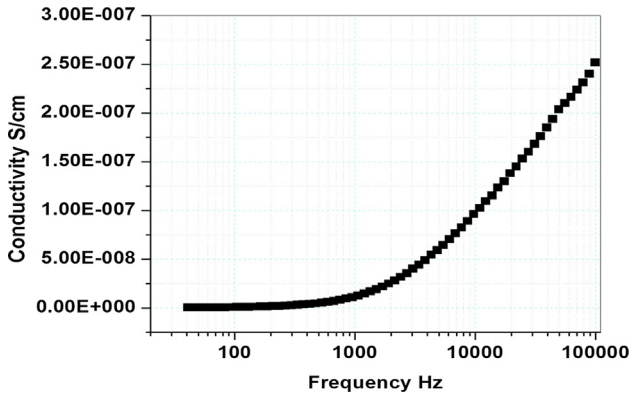


**Fig. 15.** The relation between conductivity (σ) and frequency Hz at room temperature for sample M3.

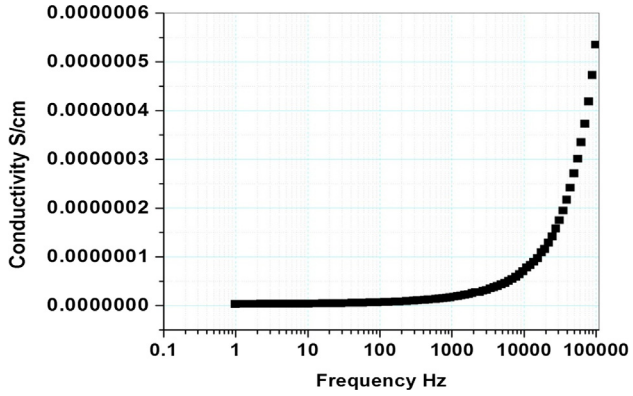


**Fig. 16.** The relation between conductivity and frequency at room temperature for sample M5.

## 3. Conclusion

SEM and AFM revealed the presence of inter-granular phase and the additives present in grain boundaries between ZnO grains. All samples contain carbon, the CuO in M2 sample wasn't detected by EDX as its percentage is as low as 0.3 mol% which is a minimum limit for EDX to detect. CuO additives produce change in the grain size and surface roughness. Increasing the concentration of CuO leads to increase of the conductivity above the breakdown frequency which is about 1 KHz. The conductivity and the dielectric constant are highly dependent on the CuO dopant amount, surface morphology, and microstructure of ZnO varistor. There are two models postulated to describe the microstructure of ZnO depending on constitution; the three phase model comprising grains, intergranular material, and particles, and the two phase model comprising the first two only. The addition of CuO leads to a two phase microstructure; well crystalline ZnO grains showing grain growth in preferred orientation, ZnO crystallizes in hexagonal system; it is characterized by prefect cleavage plane along (0 0 1) which was distinct in SEM of ZnO with different additives.

## References

Gupta, T.K., 1840. J. Am. Ceram. Soc. 73, 1990.
Vandal Pol, F.C.M., 1990. Am. Ceram. Soc. Bull. 69 (12), 1959–1965.
Clarke, D., 1999. Varistor ceramics. J. Am. Ceram. Soc. 82 (3), 485–502.
Greuter, F., Blatter, G., 1990. Semicond. Sci. Technol. 5 (2), 111–137.
Matsuoka, M., 1971. Jpn. J. Appl. Phys. 10, 736.
Matsuoka, M., Masuyama, T., Ida, Y., 1970. Suppl. J. Jpn. Soc. Appl. Phys. 39, 94.
Yoshitsugu, T., Takeshi, M., Eishitanaka, 1988. J. Am. Ceram. Soc. 71 (5), 391–395.
Steele, P.C.H., 1993. Appl. Sci. 1 (Elsevier, Chapter (1) ZnO-Varistors A. Iagrange).
Machlen (Ed.), 1979. Thermistors. Electrochemical Publications, Ltd., Ayr, Scotland.
Chiou, Bi-Shiou, Ji, F.W., 1986. Br. Ceram. Trans. J. 85, 118–122.
Cerva, H., Russwurm, W., 1988. J. Am. Ceram. Soc. 71 (7), 522–530.
Jokemura, Kobayashi, M., Takada, Y., Sata, K., 1986. J. Am. Ceram. Soc. 69 (5), 430–436.
Levinson, L.M., Philipp, U.R., 1975. J. Appl. Phys. 46, 1332.
Desouky, Osama A., 2015. Dielectric properties of ZnO 99-X $Bi_2O_3$ 0.5 CoO0.25Cr2O3 0.25 Ce6O11 X ceramics. Int. J. Adv. Res. 3 (10), 1785–1791.
Saadeldin, M.M., Younis, M.M., Ahmed, M.M., Helali, M.Y., 2015. The effect of firing temperature on the electrical properties and the microstructure of ZnO varistors doped with CuO. Indian J. Appl. Res. 5 (10).